Machinability of Gray Cast Iron: A Drilling Study

C.M. Burke
D.J. Moore
J.R. Parolini
K.B. Rundman
Michigan Technological University
Houghton, Michigan
D. Waarala
Grede Foundries
Kingsford, Michigan

ABSTRACT

C-bars of gray cast iron from nine different cupola-based heats were cast into nobake sand molds and then shaken out at a variety of temperatures and times. Alloy variations included carbon equivalence and the selection of various amounts of alloying elements. Shakeout temperatures were made consistently for each heat by the inclusion of thermocouples in the centers of each C-bar. Cooling curves were obtained for the entire temperature interval between solidification and including the pearlite reaction for each alloy and shakeout condition.

A drilling study was carried out on the cross section of each C-bar in which a new titanium nitride coated drill bit was used for each specimen. Holes were drilled for a constant time at a constant drill speed with a constant load on the drill press spindle. The weight loss during drilling was taken as a measure of the machinability.

It was shown that the machinability increased with decreasing shakeout temperature, decreased marginally with certain alloy additions and decreased significantly in heavily alloyed irons or in lower carbon equivalent irons, and increased significantly as the graphite fineness increased. X-ray diffraction analysis was used to estimate the amount of iron carbide present in the pearlite. Scanning electron microscopy and optical metallography were used to evaluate the fineness of the pearlite.

INTRODUCTION

The machinability of gray cast iron is generally quite good because of the presence of near continuous graphite flakes in the microstructure. The flakes' presence promote chip formation,[1] as well as lubrication during the machining operation. Despite this generally good response to machining, situations exist where the relative machinability from one batch of castings to another may vary considerably. This machinability variation is usually measured by changes in tool life, power requirements, volume of material removed prior to tool failure, surface finish and accuracy, or even a change in the number of castings machined per tool. Sometimes these variations in machinability occur without obvious changes in microstructure, a dilemma for the foundry trying to produce uniform microstructures, from heat to heat.

Microstructural factors having an effect on the machinability (in addition to the presence of graphite) include variations in the austenite decomposition products or the presence of other phases like eutectic carbides,[2] titanium nitrides, slag and sand. Austenite decomposition products include pearlite, free ferrite, ausferrite (bainite-like acicular product) or any combination of these products. The presence of eutectic carbides may result from inadequate inoculation in thin sections. This constituent is especially harmful to cutting tools, especially when it is present in amounts greater than 5%. In heavier-section castings that have been well inoculated, this is not usually a problem.

Variations in austenite decomposition products in unalloyed irons can include variations in pearlite spacing and/or variations in the amount of lamellar iron carbide within the pearlite, so-called microcarbides.[3] This amount of pearlitic iron carbide can vary with alloy content or by changing the shakeout temperature and time of the castings. In addition to these variations in spacing and amount of pearlitic carbide, there is always the possibility of the formation of free ferrite on the existing graphite, depending upon the cooling rate, the alloy content and the relative fineness of the graphite flakes. Most applications for as-cast gray iron specify at least 95% pearlite with random A-type graphite flakes, a microstructure that optimizes the properties of strength and machinability.

Bates' recent work on the machinability of gray cast iron[3] was done by measuring flank wear, in drilling experiments conducted on plate castings produced by a number of foundries. In that work, measurements of the volume percent of microcarbides present in the irons were related to the wear rate. It was observed that, when the volume fraction of microcarbides exceeded 11.5%, the wear rate increased dramatically.

There have been some attempts to relate the machinability of gray cast irons to the microstructure of the castings, one being the work of Moore and Lord.[4] That work used quantitative metallographic techniques to describe the microstructure and then used multiple linear regression to write an equation for machinability, M:

$$M = 195.5 - 1.26\ V_p + 11.7\ V_G + 1.2\ S_G$$

where V_p is the volume fraction of pearlite
V_G is the volume fraction of graphite
S_G is the size of the graphite in microns

Another important phase affecting the machinability of gray irons is manganese sulfide. Ericson and Hardy[5] demonstrated that MnS inclusions extended tool life, and that, therefore, cupola irons, with their higher S content, had somewhat better machinability than electric furnace iron.

The purpose of this work is to explore, in a consistent manner, how foundry processing variables (alloying element content, carbon equivalent (CE) and shakeout temperature and time) affect the microstructure and machinability of gray cast iron. In this work, the machinability is described in terms of the weight loss on drilling these cast irons, using titanium nitride-coated drill bits in a drill press, using a constant load and a constant drilling time. The weight loss under these conditions is inversely proportional to the machinability. This was designed to be a survey experiment, one in which practical variations in foundry processing variables were used in generating a variety of gray cast irons with mostly pearlitic microstructures.

Table 1.
Alloy Compositions

Alloy	Weight Percent												
	C	Si	Mn	S	P	Cr	Mo	Ni	Cu	Sn	Sb	Al	Ti
A 3#/T FeSi	3.4	**1.94**	0.6	0.109	0.04	0.134	0.083	0.08	0.27	0.027	0.01	0.006	0.02
B 3#/T SS	3.35	**1.91**	0.59	0.104	0.038	0.129	0.076	0.08	0.254	0.026	0.009	0.006	0.02
C 3#/T FeSi	3.34	**1.97**	0.6	0.113	0.039	0.12	0.074	0.07	0.24	0.024	0.006	0.004	0.017
D C+.05 Sn	3.38	**1.96**	0.6	0.11	0.039	0.12	0.074	0.07	0.25	**0.071**	0.006	0.004	0.017
E C+.02Sb	3.33	**1.88**	0.58	0.112	0.039	0.12	0.077	0.07	0.25	0.024	**0.026**	0.004	0.016
F Base	3.38	1.77	0.58	0.111	0.04	0.12	0.073	0.07	0.24	0.024	0.007	0.004	0.016
F C+.11 Cr	3.37	**1.94**	0.59	0.112	0.04	**0.23**	0.073	0.07	0.25	0.024	0.007	0.005	0.017
G 3#/T FeSi	**3.11**	**2.34**	0.65	0.105	0.042	0.15	0.078	0.08	0.31	**0.07**	0.008	0.004	0.019
H 3#/T FeSi	**2.87**	**2.5**	0.66	0.107	0.042	0.15	0.079	0.08	0.31	0.025	0.008	0.004	0.019
I C+CuCrMo	3.37	**1.96**	0.63	0.116	0.043	**0.23**	**0.39**	0.08	**0.55**	0.022	0.008	0.007	0.02

EXPERIMENTAL PROCEDURE

Nine different alloys were produced from cupola iron by either alloying and inoculating directly from the large holding furnace, or (in the case of the two low-CE irons) by a special melting and casting arrangement with the small induction furnace.

The chemical compositions of the final inoculated irons are given in Table 1. In Table 1, the numbers in bold indicate the departure of that particular alloy from the normal base iron. It will be noted that Alloys A and C are normal base irons inoculated with 3 lb/ton of foundry grade ferrosilicon, while Alloy B is a normal base iron inoculated with Superseed.

Alloys D, E, F, G, H and I have been inoculated with 3 lb/ton of foundry grade ferrosilicon and alloyed in the ladle with different combinations of Sb, Sn, Cr, Cu and Mo. Alloys G and H are low-CE irons with carbon content lower than the normal base iron and silicon content higher than the normal base iron.

Standard C-bar molds, prepared in a nobake sand, half of which contained a thermocouple placed in the center of the 2x8-in. (5.1x20.3 cm) long bar, were poured in a sequence indicated in Table 2. Alloys A and B were the first poured, and the strict schedule adopted for shakeout in later heats was not followed.

Table 2 indicates that most of the castings, Alloys C through I, were shaken out in the order: 1600F (871C), 1400F (760C), 2 min after the beginning of the pearlite transformation (BPT) and 6.5 min after the BPT. (In this instance, the beginning of the pearlite reaction was taken as that point in time when the temperature had reached a minimum, prior to the pearlite reaction, see Fig. 1.) The exceptions to this schedule for Alloys A and B are noted in Table 2. The scenario finally adopted for shakeout in the heats C through I is illustrated in the schematic cooling curve in Fig. 1. Actual cooling curves for some of these castings, in which successful data was obtained, are shown in the Appendix.

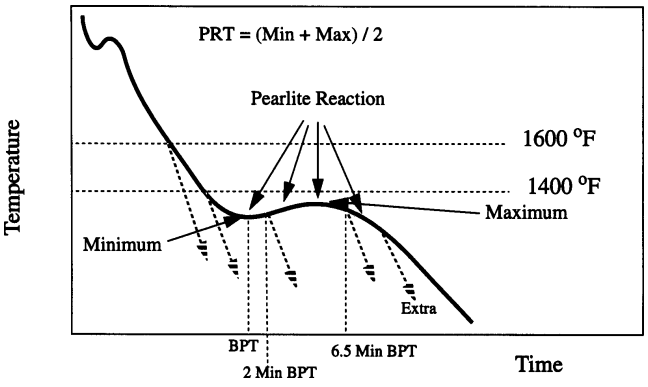

Fig. 1. Schematic cooling curve illustrating the shakeout sequence.

TENSILE STRENGTH AND HARDNESS

The C-bars were poured in duplicate, with one of each being used for tensile and hardness measurements and the other (the one with the thermocouple) for microstructural analysis and machinability testing. Each non-thermocoupled C-bar had a single tensile bar machined from it, and had two hardness measurements made: one on the casting surface and one on the interior. The tensile and hardness results are recorded in Table 3. This table includes hardness results from the interior of thermocoupled bars, which also were machinability tested. As expected, the hardness and tensile strength of the bars decreased as the shakeout temperature decreased. A graphical summary of the Brinell hardness number (BHN) vs. shakeout strategy is shown in Fig. 2.

Table 2.
Identification of Shakeout Conditions

Alloy	Specimen Identification Scheme			
	Shaken Out at 1600 °F	Shaken Out at 1400 °F	Shaken Out at 2 Min After BPT*	Shaken Out at 6.5 Min After BPT
A	A0	A1	A2 (SO at 1300)	A3 (SO at 1200)
A**		A4	A5 (SO at 1300)	A6 (SO at 1200)
B	B0	B1	B2 (SO at 1340)	B3 (SO at 1300)
B**		B5 (SO at 1390)	B6 (SO at 1340)	B4 (SO at 1300)
C	C0 (SO at 1800)	C1	C2	C3
D	D0	D1	D2	D3
E	E0	E1	E2	E3
F	F0	F1	F2	F3
G	G0	G1	G2	G3
H	H0	H1	H2	H3
I	!0	I1	I2	I3
* BPT = Begining of Pearlite Transformation				
** Let Melt Fade in Ladle for 8 Minutes before Pouring Castings				

The effect of alloy additions can be clearly seen in Fig. 2. The highly Alloyed I casting has the highest hardness values for all shakeout conditions; and the normal base iron, Alloy C, has the lowest hardness. Irons alloyed with Sn, Sb and Cr show slightly higher hardnesses than the plain irons. Low-CE irons G and H fall in between the lightly alloyed irons and the heavily alloyed I.

The variation of ultimate tensile strength (UTS) with BHN (measured internally) is plotted in Fig. 3. In addition to the data from each C-bar, the ratios of UTS to BHN are also included as lines on Fig. 3. It can be seen from Fig. 3 that a large variation in tensile data was observed in the experiment, and that the relationship to Brinell hardness was a normal one. This large variation provides a good variation over which to test the machinability of these irons.

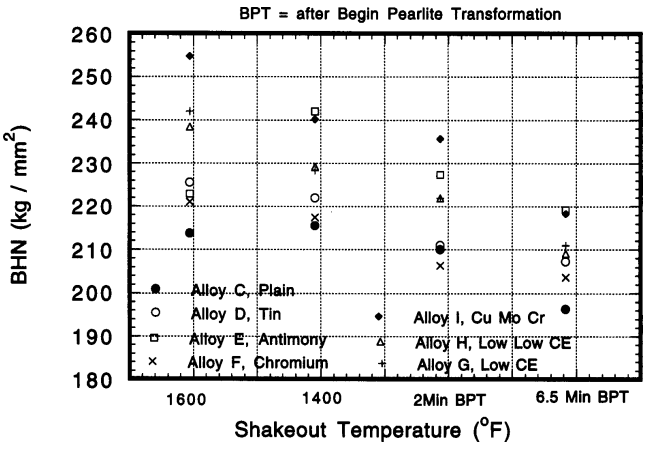

Fig. 2. Internal BHN vs. shakeout temperature.

Table 3.
Ultimate Tensile Strength and Brinell Hardness

Alloy	UTS	BHN (kg/mm^2)			Alloy	UTS	BHN (kg/mm^2)		
	ksi	In	Out	MTU		ksi	In	Out	MTU
A0	47.1	241	187	189	B0	38.3	208	217	197
A1	36.6	181	217	186	B1	37.4	201	217	194
A2	34.7	180	207	178	B2	36.7	184	197	187
A3	31.8	183	179	172	B3	34.6	180	187	181
A4	32.7	179	179	182	B4	34.7	195	217	194
A5	33.7	190	207	177	B5	32.7	191	207	168
A6	30.3	176	179	168	B6	26.7	176	179	187
C0	34.4	207	196	198	D0	37.1	220	207	215
C1	33.9	209	187	197	D1	37.8	216	207	203
C2	33.9	203	179	189	D2	37.1	204	196	197
C3	32.0	188	170	179	D3	31.7	200	187	188
E0	36.1	217	217	221	F0	41.1	215	207	206
E1	36.9	238	217	217	F1	38.7	211	202	207
E2	37.1	222	207	207	F2	36.3	199	196	190
E3	35.9	213	207	191	F3	34.8	196	179	186
G0	36.0	238	262	221	H0	40.2	234	262	224
G1	36.4	223	241	210	H1	38.9	224	241	213
G2	33.6	216	235	202	H2	35.9	216	228	209
G3	33.6	204	223	193	H3	34.6	202	212	196
I0	43.5	252	262	239					
I1	46.4	236	255	234					
I2	42.9	231	241	209					
I3	40.2	212	223	199					

Machinability Testing by Drilling

The primary objective of this the work was to evaluate the machinability of the irons of Table 1 for the processing conditions indicated in Table 2, and then to relate machinability to the microstructural features of the gray cast iron, and, more specifically, the machinability involved in drilling. The drilling test was selected because a significant fraction of the machining of gray iron involves drilling or boring. In addition, the group at MTU had some previous experience in using the drilling test. A schematic of this test is shown in Fig. 4, together with a specimen shown to scale.

The schematic in Fig. 4 illustrates the setup used for drilling and obtaining Brinell hardness measurements, holes being drilled at points 1/2, 3/4 and 7/8 in. (1.27, 1.91 and 2.22 cm) from the center of the 2-in. (5.1-cm) dia bar. Each new specimen was begun with a new drill bit. Work with the titanium nitride-coated drill bits indicated that the drill bits wear very little in drilling one specimen (from 20–30 holes per specimen). Therefore, any variations in machinability should be a result of the influence of the microstructure. It was implicitly assumed that each new drill bit would be identical to one another. The pattern of holes and Brinell measurements suggested in Fig. 4 illustrates the desire to obtain Brinell hardness measurements as close to the drilled material in the 1/2 radius and 3/4 radius position as possible. It was not possible to obtain BHN measurements at the 7/8 position.

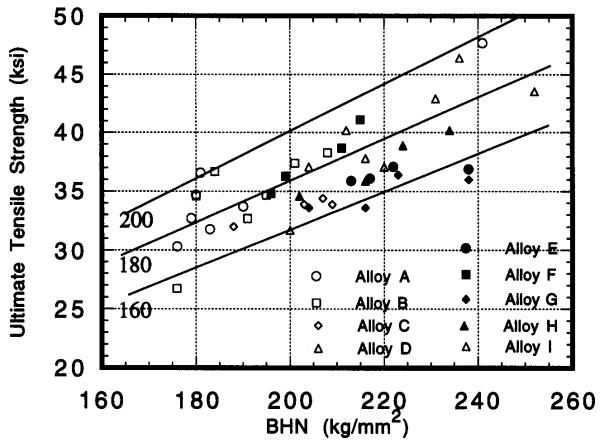

Fig. 3. UTS vs. BHN from C-bars, internal hardnesses; lines are ratios of UTS (in psi) to BHN.

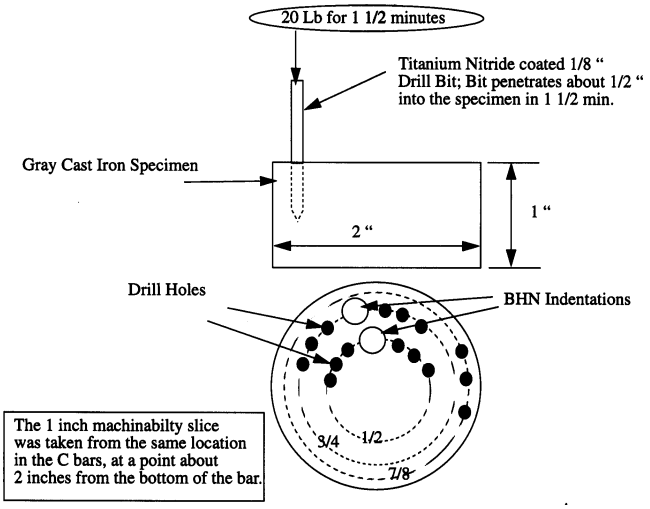

Fig. 4. Schematic of machinability test apparatus.

Measurements involved weighing the specimen before testing began, and then weighing again after drilling three holes. In every instance, the pattern of drilling was as follows: three holes were drilled first at the 3/4 radius followed by three holes at the 1/2 radius. This procedure was continued until at least nine holes were drilled at each radius, the data being recorded as a weight loss in grams. All of the data at the 7/8 radius was collected after the data at the 3/4 and 1/2 radii were completed. Each measurement at each radius was then averaged for the three sets of three-hole weight loss data. This weight loss data is recorded in Table 4.

Table 4.
Weight Loss Measurements and S_V Data

Specimen	Weight Loss (Grams)			S_V (mm^{-1})		
	1/2 "	3/4 "	7/8 "	1/2 "	3/4 "	7/8 "
A0	2.85	2.98	3.03	26.7	37.6	37.6
A1	2.30	2.43	3.05	26.3	29.7	36.5
A2	2.81	3.00	3.32	27.8	27.8	35.7
A3	3.26	3.52	3.73	29.3	33.1	35.7
A4	4.16	4.43	4.46	36.8	41.3	53.8
A5	2.92	3.12	3.34	38.0	36.5	40.2
A6	3.00	3.29	3.92	35.0	39.1	42.1
B0	2.49	2.72	2.64	29.7	31.6	38.0
B1	2.85	3.01	2.88	26.3	33.1	36.5
B2	3.29	3.48	3.68	28.6	35.9	49.2
B3	2.11	2.32	3.33	26.1	28.8	44.0
C0	2.12	2.48	2.65	31.2	37.2	32.7
C1	2.49	2.79	2.93	22.9	25.9	28.9
C2	2.92	2.94	3.16	30.1	34.6	34.6
C3	2.87	3.06	3.11	26.7	27.8	28.6
D0	2.76	2.87	2.83	27.4	32.0	37.6
D1	2.82	3.03	2.87	28.6	38.4	41.4
D2	2.94	3.03	3.19	30.8	39.1	32.3
D3	3.29	3.49	3.58	25.2	39.1	34.6
E0	2.43	2.57	2.48	34.2	35.4	42.1
E1	2.60	2.70	2.48	30.8	40.6	36.8
E2	2.53	2.59	3.13	27.6	35.7	36.8
E3	3.16	3.20	2.63	34.6	35.7	36.8
F0	3.01	3.09	2.99	30.8	40.2	32.3
F1	3.37	3.49	3.5	34.4	41.4	31.8
F2	2.81	2.94	2.91	30.8	31.6	34.2
F3	2.65	2.83	2.84	33.5	33.5	36.1
G0	2.67	2.91	2.88	34.0	33.3	41.7
G1	2.17	2.36	2.34	24.8	33.5	27.1
G2	2.34	2.60	2.76	28.2	31.6	34.2
G3	2.79	3.01	3.15	27.4	32.7	30.4
H0	1.88	2.16	2.28	26.9	33.3	36.1
H1	2.11	2.32	2.55	24.1	28.9	27.1
H2	2.58	2.82	2.86	25.6	22.6	25.6
H3	2.65	2.94	3.05	26.3	25.6	32.3
I0	1.53	1.7	1.71	18.8	16.5	30.1
I1	2.21	2.3	2.45	25.6	24.8	28.6
I2	2.42	2.61	2.53	22.9	33.1	33.1
I3	2.88	3.04	2.93	28.6	28.9	33.1

Metallography

A metallographic specimen was obtained from each bar, as shown in Fig. 5. Specimens in the unetched condition were used to evaluate the graphite surface area per unit volume (S_V) and in the etched condition to verify the matrix microstructure. The specimens were mostly pearlitic, there being less than 5% free ferrite in any one of the specimens.

Photomicrographs were taken at 500X in the etched condition to reveal the pearlitic appearance; i.e., coarse vs. fine. Scanning electron microscopy (SEM) was used to evaluate the fineness of the pearlite and to obtain an estimate of the pearlite spacing in several of the alloy specimens. The method used to estimate S_V at 1/2, 3/4 and 7/8 is illustrated in Fig. 5. Unetched specimens were used to measure the S_V of the graphite at the 1/2, 3/4 and 7/8 positions. These data are recorded in Table 4.

X-Ray Diffraction

The x-ray diffraction technique has been used to obtain an estimate of the amount of carbide present in the pearlite. This was done by first doing diffraction work on four plain carbon steels that have varying amounts of carbon (measured by LECO analysis) and, therefore, varying amounts of iron carbide.

Diffraction scans were obtained from four plain carbon steel standards and six of the alloys studied here in two shakeout conditions: the highest shakeout condition (1600F/871C) specimens of Alloys A, D, E, F, H and I, and the latest time shakeout condition of each alloy. Each diffraction scan provided quantitative information about the phases that were present.

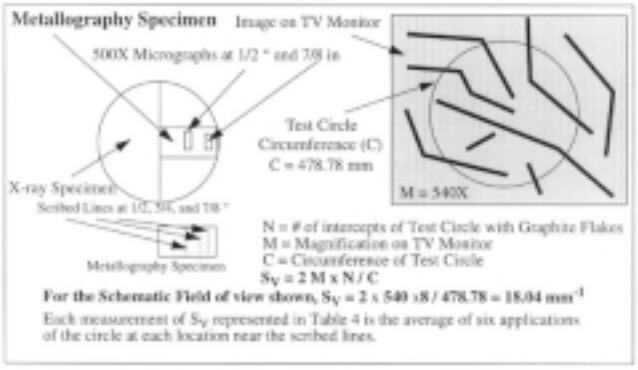

Fig. 5. Schematic illustrating the section selected for metallography and S_V measurement.

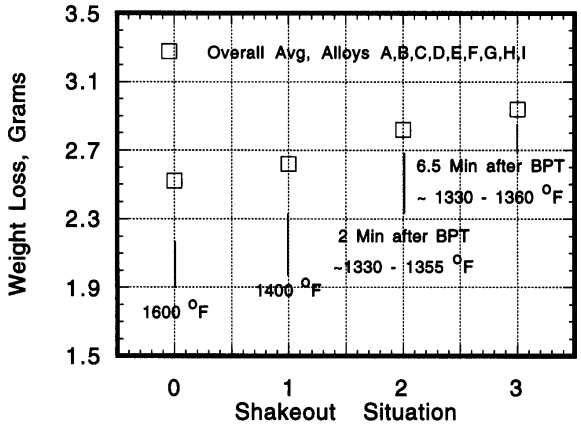

Fig. 6. Weight loss vs. shakeout situation.

EXPERIMENTAL RESULTS AND DISCUSSION

Weight Loss Data

Dependence of Weight Loss on Shakeout Temperature

The weight loss data of Table 4 represents a measure of machinability. The larger the weight loss, the better the machinability of the iron. It can be seen on examining the data in Table 4 that the weight loss, in general, increased as the shakeout temperature decreased. This can be seen in Fig. 6, a plot of averages for all alloys and positions in the casting. This is a result generally expected from the behavior of BHN vs. shakeout situation reported in Fig. 3; i.e., one would expect that the machinability would decrease with increasing hardness. This result gives weight to the idea that improving machinability would result by leaving the castings in the mold as long as possible before shakeout. The data of Fig. 6 imply that leaving the casting in the mold to at least the end of the pearlite reaction would increase the machinability by about 16%, on average, over shaking out hot (1600F/871C).

Dependence of Weight Loss on Hardness and Alloy Content

The data presented in Fig. 6 is an average result from data from all the alloys. Individual data from each alloy shows considerable scatter. This is represented in Fig. 7, a graph of weight loss vs. BHN for all of the alloys studied. (Each data point represents averages of weight loss data at 1/2 and 3/4 from the center). It can be seen in Fig. 7 that the maximum variation in weight loss is much larger than the averages plotted in Fig. 6. Figure 7 shows a variation from about 1.6 grams for the smallest value of weight loss (poorest machinability) to a high of about 3.4 grams for the highest value of machinability, an increase of over 100%. Of course the lowest machinability (1.6 grams) was associated with the alloy with the largest amount of alloying elements (Alloy I) shaken out at the highest temperature (1600F/871C).

Clearly, there is much scatter in the measured values of machinability as shown in Fig. 7. However, it appeared that, on average, the heavily alloyed irons had lesser values of weight loss. Figure 8 shows the average of all weight loss data for each alloy, at all positions in the bar and for each shakeout condition. It can be seen in Fig. 8 that the unalloyed irons, as well as those alloyed with small quantities of Sn, Sb or Cr, had quite similar machinabilities. However the low-CE irons and Alloy I containing high Cr, Mo and Cu had

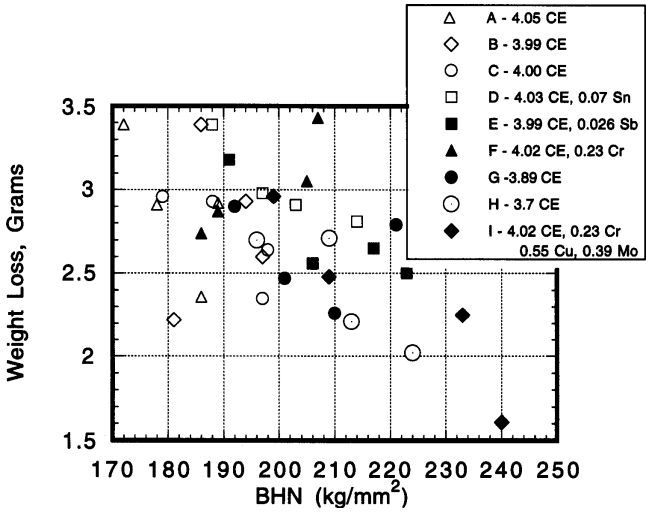

Fig. 7. Weight loss vs. BHN for all alloys studied (avg. of 1/2 and 3/4 data).

lesser machinabilities, the machinability of I being almost 25% less than that of the unalloyed irons. The machinabilities of the low-CE irons are shown to be somewhat in between that of the unalloyed condition and Alloy I.

Dependence of Weight Loss on Position in the C-Bar

It was observed during the weight loss measurements at 1/2 and 3/4 from the center of the bar that the weight loss was virtually always greater at the 3/4 position than at the 1/2 position (See Table 4), and even greater at the 7/8 position. Examination of the microstructure of these bars showed that, in almost every instance, the matrix was the same, nearly all pearlite, but that the graphite flake size was smaller at the 3/4 position and even smaller at the 7/8 position. This is consistent with the fact that solidification occurs more rapidly at distances closer to the surface of the C-bar.

The graphite flake size at 1/2, 3/4 and 7/8 was quantitatively evaluated using the intercept method, a technique where a circle is superimposed on the unetched structure and the number of intercepts with the graphite is measured. See Fig. 5 for the method used to determine S_V. It follows that more flakes will give more intercepts with the test circle, thereby giving a larger S_V. Figure 5 includes a sketch of where the intercepts were measured at six locations along each scribed line on the metallographic specimen at 1/2, 3/4 and 7/8. The S_V results are given also in Table 4.

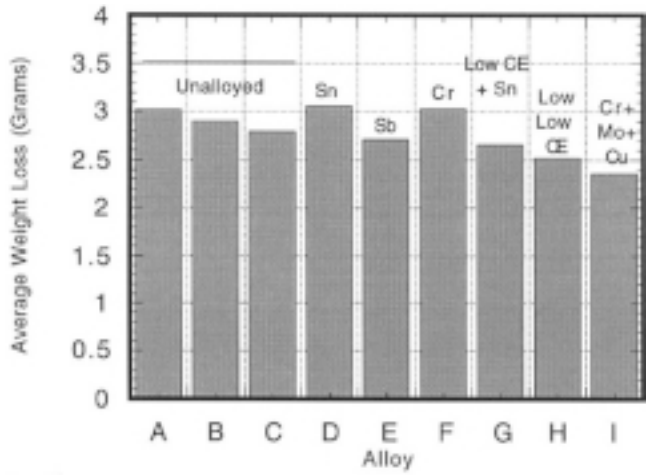

Fig. 8. Average weight loss for each alloy (each bar represents the average of 36 weight loss measurements from 108 drill holes).

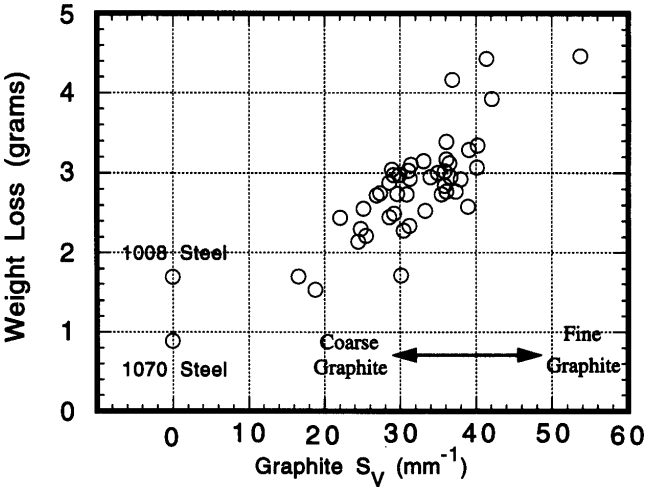

Fig. 9. Weight loss vs. measured graphite S_V for these alloys and for two plain carbon steels.

Figure 9 shows a plot of weight loss vs. S_V for all of the specimens at each distance. In addition, for comparison purposes, the weight loss was also measured in two plain carbon steel alloys: a 1008 steel, which is nearly all ferrite; and a 1070 steel, which is nearly all pearlite. Of course, the steel does not contain any graphite and so it has an S_V value of 0 and, therefore, very much reduced machinability.

It can be seen from the data of Fig. 9 that the fineness of the graphite is a very important parameter in defining the machinability of gray cast iron. This is not a surprise. The surprise to these researchers was how very rapidly the weight loss increased with increasing S_V (finer graphite). The importance of the amount of free ferrite on machinability can be inferred by noting the difference between the 1008 steel (almost all ferrite) and the 1070 steel (all pearlite). The 1070 steel is quite similar in structure to the gray cast irons of this study, in that they are almost totally pearlitic. Thus, the only microstructural difference between the 1070 steel and the gray irons is the amount and size of the graphite.

It was of interest to examine these data for a high shakeout temperature and as a function of alloy content. Figure 10 shows averages of weight loss for certain groups of alloys plotted vs. the measured values of S_V. The dashed ellipse in Fig. 10 encircles average data from alloys that were treated normally in processing. They were all inoculated and then poured off as soon as possible.

Alloy A Bar 4 (A4) was one of the bars poured after the iron had been allowed to sit in the ladle for 8 min; i.e., the melt inoculant had been allowed to fade before pouring the castings. The result for A4 was a bar with very fine graphite (a lot of D- and E-type graphite), especially at the 7/8 position. Thus, the fine graphite and the presence of ferrite combined to give the highest value of weight loss measured at 4.46 grams, with also the highest value of S_V (53.75 mm^{-1}).

This high machinability indication was observed despite the high shakeout temperature, implying that the graphite fineness overrides the tendency to reduce machinability as a result of the fine pearlite generated in hot shakeout. The straight lines through the 1070 steel at 0 S_V in Fig. 10 indicate that the weight loss data are very well behaved with increasing S_V. This graph shows that an increase in S_V of 10 mm^{-1} will increase machinability by about 20–25%. Since these differences most certainly exist in most gray iron castings, it is to be expected that machining will be easier in one part of the casting than in another, simply because of the variation in graphite size.

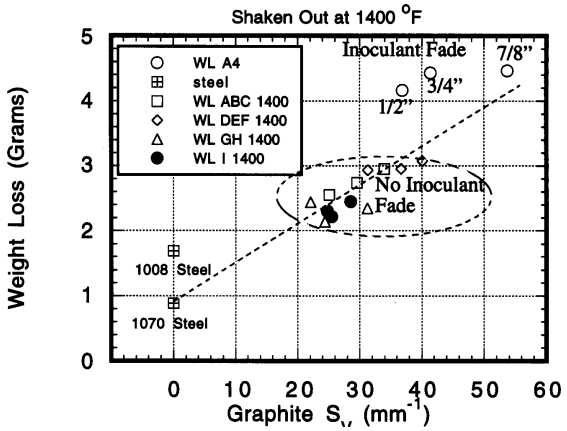

Fig. 10. Weight loss vs. S_V for averages of alloy groups. Averages are of the data obtained at 1/2, 3/4 and 7/8. These positions are shown for A4.

Effect of Shakeout Temperature and Alloy Content

One of the factors that has an impact on the machinability of gray cast iron is the shakeout temperature. Figure 6 shows the overall increase in machinability as the shakeout temperature decreases. The other factor of significance is the alloy content as shown in Fig. 8. These two process variables have an effect on the matrix microstructure, both being used to promote pearlite and increase the fineness of the pearlite that is present. It was of interest in this work to examine these effects on the cooling curves and on the pearlite fineness and carbon content. Pearlite fineness issues are being dealt with by optical metallography and by SEM microscopy. Carbon content of the pearlite issues are being addressed by x-ray diffraction.

Cooling Curves—Two of the cooling curves obtained from this study are presented in the Appendix. The most important variable measured with these cooling curves was the temperature at which the pearlite reaction temperature occurred. Figure 1 illustrates the thermal arrest corresponding to the pearlite reaction. All of the cooling curves measured showed significant undercooling and then recalescence during the time when the pearlite reaction is occurring. This recalescence is a measure of the amount of heat being released as a result of the pearlite reaction of austenite going to pearlite. An estimate of the pearlite reaction temperature was obtained from the cooling curves. This was taken to be the average of the minimum and the maximum temperatures, as shown in Fig. 1. The results of these measurements from the cooling curves are summarized in Fig. 11.

Pearlite Fineness—In reviewing the data of Fig. 11, it is important to keep in mind that, the lower the pearlite reaction temperature (PRT), the finer the pearlite. Thus, one should expect very fine pearlite in the specimens of Alloy I, the most highly alloyed iron studied. In fact, estimates of the percentage of pearlite that is too fine to resolve at 500X have been made from photographs taken of a number of the alloys shown in Fig. 11. The estimates of the percentage of fine pearlite are given in Fig. 11. All of the irons shaken out at either 1600 or 1400F (871 or 760C) have estimated values of the amount of fine pearlite in excess of 75%, an amount that is generally not considered desirable for machinability purposes. Those alloy specimens that have been shaken out at one of the later times have much lower estimates of percent fine pearlite, most being less than 50%. Examination of photographs at 500X for the amount of fine pearlite is a very subjective measurement, the results varying greatly from one person to the next.

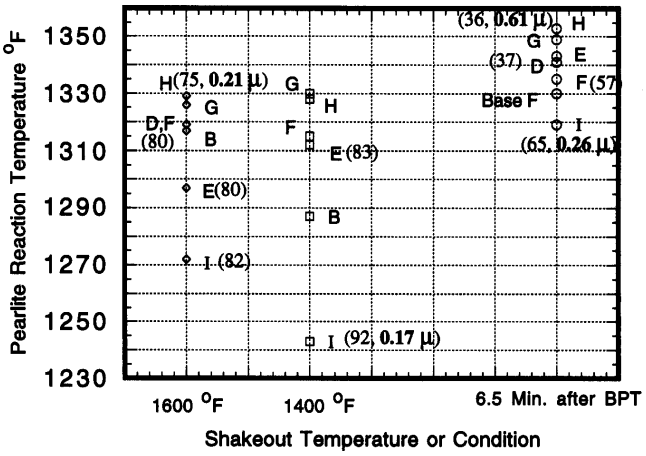

Fig. 11. Pearlite reaction temperature vs. shakeout temperature or condition for a number of alloys with successful cooling curves. Numbers in ( ) are the estimated percent fine pearlite at 500X. Bold numbers are the pearlite spacings in microns measured by SEM.

SEM of Selected Specimens—This work has also made an attempt to measure the pearlite spacing using SEM, a very difficult measurement because of the fineness of the pearlite and the nature of the measurement. Approximately one dozen specimens from the C-bar castings were examined by SEM at a magnification of 10,000X. In this work, the specimens were scanned until the operator found the finest spacing pearlite, and this was photographed and the spacings were measured. This spacing was then taken to represent the true spacing of the pearlite present, assuming that all of the pearlite in the specimen had the same spacing, and the finest spacing pearlite would be that whose plates were oriented perpendicular to the surface.

Estimates of the pearlite spacing from individual photographs give 0.17, 0.26, 0.21 and 0.61 microns for Alloys I1, I3, H0 and H3, respectively. These numbers are consistent with other measurements on pearlite spacings in irons and steels. These numbers are also indicated in Fig. 11. Notice in Fig. 11 that the largest pearlite spacing occurred in the slowest cooling unalloyed specimen (H3) in which pearlite formed at the highest possible temperature. The smallest pearlite spacing occurred in the most highly alloyed and very rapidly cooled iron shaken out at 1400F (760C) (I1) in which the pearlite formed at the lowest possible temperature.

Amount of Carbon (Carbide) in Pearlite—Diffraction scans were made on each of 12 specimens of two carbide peaks. The integrated intensities of the carbide peaks were used to estimate the amount of carbon (and, therefore, carbide) in the pearlite in each iron. The sum of the integrated intensities of the two carbide peaks for the four standards (1045, 1053, 1070, 1095) is shown in Fig. 12, together with the straight line fit through 0 wt% carbon. A similar measurement on the 12 cast irons will result in a measurement of the intensity of carbide in the irons. This intensity can then be translated to the amount of carbon present in the pearlite in the iron by extending the measured intensity on the y-axis to the standard line and then reading off the amount of carbon on the x-axis.

Figure 12 illustrates that the major difference between the two different groups of specimens is that the specimens shaken out at 1600F (871C) have a higher average carbon measurement than those specimens shaken out late in the process. This difference of ~0.17

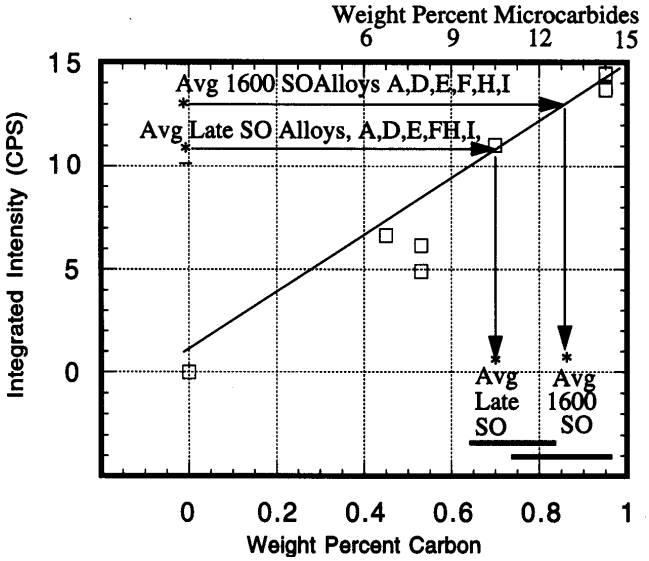

Fig. 12. Sum of the integrated intensities of carbide peaks vs. wt% C. Data points from plain C normalized (air cooled after austenitization) steel specimens.

wt% C is consistent with the notion that the wt% C will decrease in the matrix austenite during cooling of the casting. Castings shaken out at 1600F (871C), however, will cool fast enough that the carbon content cannot keep pace with the requirements of the phase diagram and will, therefore, have more C than the more slowly cooled castings.

Since more C in pearlite means more carbide (% carbide = 14.9625 x wt% carbon) and perhaps a finer scale carbide, the result for machinability is that one would expect the higher shakeout temperature irons to have lower machinability. Indeed, this is born out by the average machinability data in Fig. 6, where the lowest shakeout condition (with lowest amount of iron carbide) has machinability about 15% better than that of those castings shaken out at 1600F (871C).

Figure 12 plots the wt% microcarbide on the top x-axis for reference. It can be seen from Fig. 13, a plot of weight loss vs. percent microcarbides, that the percent microcarbides measured by this direct method spans the range 9.7–12.6 for the specimens shaken out 6.5 min after BPT, while the percent microcarbides in those shaken out at 1600F (871C) ranges from 11.07 to 14.5.

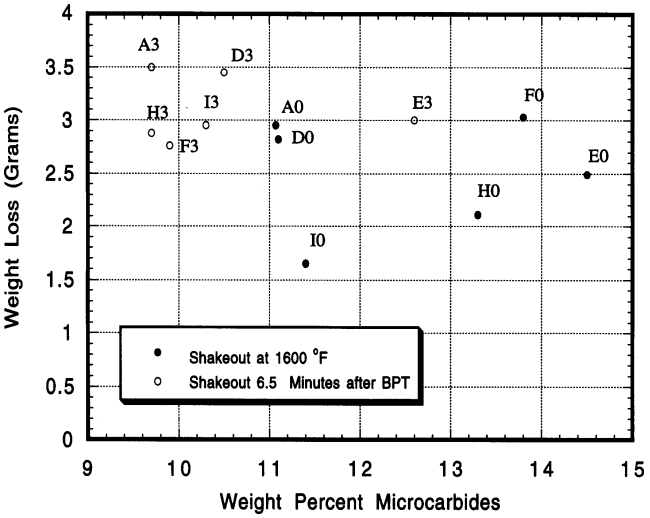

Fig. 13. Average weight loss (1/2, 3/4 and 7/8) vs. measured percent microcarbides for six alloys shaken out at 1600F (871C) and also after 6.5 BPT.

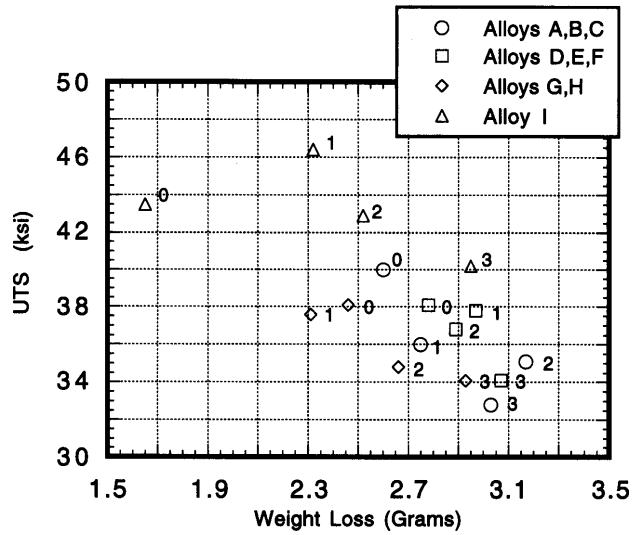

Fig. 14. UTS vs. weight loss for the alloys studied here. Numbers beside data points refer to shakeout scheme. 0–1600, etc.

Each alloy specimen is identified in Fig. 13. It is significant that Alloy E0 with an Sn addition has the highest amounts of microcarbides for both shakeout conditions. This is consistent with the understanding that tin slows carbon diffusion into and out of the graphite. As expected, there is some trend to lower weight loss as the percent microcarbides increases, but it is not a dramatic event like that described by Bates.[3] In that study, he shows that when the wt% microcarbides exceed 11.5%, the machinability (number of holes before tool failure) drops to a very low value. It is quite clear that much more data needs to be obtained before definitive conclusions can be reached.

UTS and Weight Loss

The ultimate in practical results for this casting would be to produce one with a maximum in tensile strength and a maximum in machinability. The manufacturer would like the best of both worlds. Unfortunately, these generally work in opposite directions. If the UTS is high, then, too often, the machinability is low and vice-versa. This behavior can be seen, in general, in the results of this work. Figure 14 is a plot of UTS in ksi vs. weight loss. The data were averaged for the plain alloys, ABC, and for the singly alloyed irons, DEF, and for the low-CE irons, GH. Alloy I, the most heavily alloyed iron, stands on its own. It can be seen from Fig. 14 that, as UTS increases, the weight loss generally decreases, although there is significant scatter in the data.

CONCLUSIONS

1. In this survey experiment, weight loss and, therefore, machinability (by the drilling test on C-bars) of pearlitic gray cast irons with a range of alloy compositions increases and decreases as follows:

- increases about 15% as shakeout temperature decreases from 1600F (871C) to 6.5 min after the beginning of the pearlite transformation, BPT;
- decreases about 15–25% with heavy alloy additions or by reducing CE;
- increases about 20% for every 10 mm^{-1} increase in S_V;
- increases as the amount of ferrite increases.

2. A direct method to evaluate the wt% carbides present in the pearlite gave results that were consistent with expectations. The absoluted values were in the same range as those quoted by Bates[3] for "microcarbides." The amount of these microcarbides increased as the shakeout temperature increased. The more rapid cooling experienced by the higher shakeout temperature specimens did not give enough time for the carbon to be redistributed to the graphite. Therefore, a larger carbon content and, therefore, larger carbide content was observed in the pearlite. The amount of microcarbides varied from one alloy to the next. This is to be expected because of the effect that alloying elements have on the ability of carbon to move between austenite and graphite on cooling. It was observed that the alloy with tin, Alloy E, had the largest amount of microcarbides in both shakeout conditions. This is consistent with the understanding that tin slows carbon diffusion into and out of the graphite.

3. Higher shakeout temperatures resulted in generally higher hardnesses, a result of the production of finer pearlites with a larger fraction of microcarbides.

ACKNOWLEDGMENT

The authors would like to thank the Grede Foundries Inc. for the financial support to do this work.

REFERENCES

1. J.T. Berry, R. Salame-Lama and A. Saigal, "The Machinability of Engineering Materials," *Proceedings of the ASM International Conference on the Influence of Metallurgy on the Machinability of Engineering Materials,* Rosemont IL, Sep 1982; American Society for Metals (1983).
2. J.F. Janowak, "Cast Iron Metallurgy for Improved Machinability," *Proceedings of the International Conference on High Productivity Machining, Materials and Processing,* New Orleans, LA, May 1985, Edited by V.K. Sarin, American Society for Metals.
3. C.F. Bates, "Study Examines Influences on Machinability of Iron Castings," *Modern Casting,* pp 36-39, Oct 1996.
4. W.W. Moore and J.O. Lord, "Gray Cast Iron Machinability," *AFS Transactions,* vol 67, pp 193-198 (1959).
5. P.S. Ericson and J.M. Hardy, "Effect of Manganese Sulfide Inclusions in Cast Gray Iron on Tool Life," *AFS Transactions,* vol 84, pp 407-416 (1976).

APPENDIX

Cooling Curves From Selected Alloy Specimens

Cooling curves were obtained from a number of alloy specimens—Alloys D, E, F, G, H and I—shaken out at different temperatures and times. Each curve was obtained from a thermocouple placed at the center of the C-bar. Two sets of cooling curves are given in Figs. A1 and A2. Items to note in these curves are the following:

1. The designation with a 0 means that the C-bars were shaken out at 1600F (871C). The shakeout temperature can be seen in the cooling curves where there is an obvious change in slope at about what appears to be 865C (~1590F). While the C-bar castings were shaken out at precisely 1600F (871C), in each case there is an obvious delay in the response of the center-located thermocouple to this action.
2. The designation with a 3 means that the C-bars were shaken out after nominally 6.5 minutes after the beginning of the pearlite reaction (BPT). In these instances, the curves show an obvious break at the end of the pearlite reaction at shakeout, with a rapid change in slope.
3. The relative positions of the curves show a variation in the times of the shakeout and in the pearlite reaction times. The time scale on the cooling curves is relative to the time when the computer that collected the data was turned on, and bears no relation to the actual time after pouring the casting. The important times in the shakeout sequence relative to the actual time of pouring the casting, and the actual time range over which the pearlite transformation is occurring are as follows:

(Time is in minutes)	*1600F (871C)*	*1400F (760C)*	*2 Min after BPT*	*6.5 Min after BPT*
Shakeout time (average after pouring)	17.4	25.4	31.4	36.2
Pearlite reaction time (average for Alloys D, E, F, G, H and I)	2.2	2.2	4.8	7.5

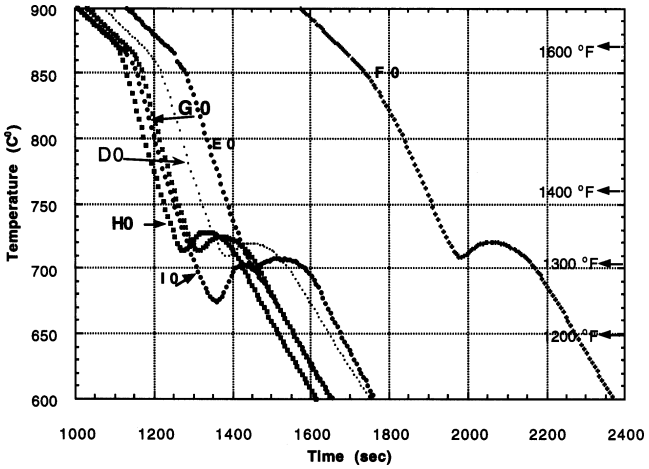

Fig. A1. Cooling curves for Alloys D–I shaken out at 1600F (871C)

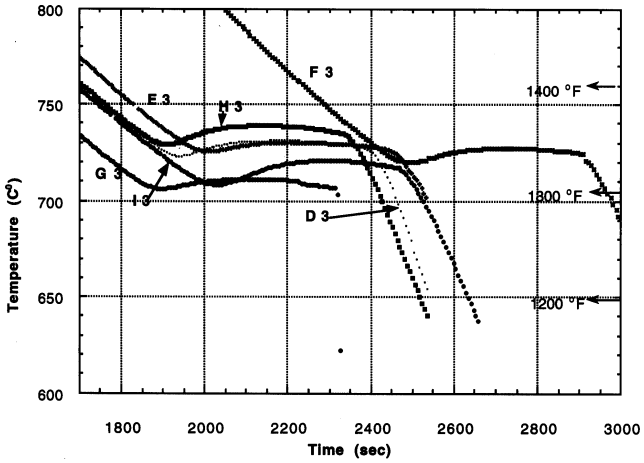

Fig. A2. Cooling curves for Alloys D–I shaken out 6.5 min after BPT.